



# Fatigue behavior of self-healing glass fiber/epoxy composites with addition of poly (ethylene-co-methacrylic acid) (EMAA)

Allana Azevedo do Nascimento<sup>a,\*</sup>, Volker Trappe<sup>b</sup>, José Daniel Diniz Melo<sup>a</sup>, Ana Paula Cysne Barbosa<sup>a</sup>

<sup>a</sup> Federal University of Rio Grande do Norte (UFRN), Av. Senador Salgado Filho 3000, CEP, 59078-970, Natal, RN, Brazil

<sup>b</sup> Federal Institute for Materials Research and Testing (BAM), Unter den Eichen 87, 12205, Berlin, Germany

## ARTICLE INFO

### Keywords:

Glass fiber-epoxy composites  
Self-healing  
Smart materials  
Fatigue

## ABSTRACT

The interest in repair technologies for polymer composites has increased significantly over the last decades, due to the growing use of these materials in structural applications. In this study, poly (ethylene-co-methacrylic acid) (EMAA) was used as self-healing agent to glass fiber/epoxy composite. Materials with EMAA contents of 2 wt% and 5 wt% were manufactured using Resin Transfer Molding (RTM) and the effects of the healing agent on the properties were investigated using tensile tests and Dynamic Mechanical Analysis (DMA). Results show slight variation of properties, which was more pronounced as the content of EMAA increased. In addition, the healing efficiency was investigated through fatigue tests and the addition of higher content of EMAA increased the number of cycles to failure after the healing activation cycle.

## 1. Introduction

Glass fiber reinforced polymers (GFRP) have been widely used for structural applications, to meet requirements of mechanical strength, stiffness, corrosion resistance, in addition to their weight savings attractiveness [1,2]. Due this combination of mechanical properties and lightweight, these composites have been the most used materials for wind turbine blades [3]. GFRP components are exposed to severe environmental variations during service, including a combination of exposure to chemicals and mechanical stresses that can cause damages as microcracks and delamination. Many of these damages are not readily detectable and can propagate rapidly, reducing performance or causing structural failure. Thus, inspection and maintenance procedures are necessary [1,3,4].

Repairs on parts that failed prematurely may incur significant extra costs and, therefore, the optimization of repair methods is considered an important task. Self-healing composite materials have been developed in the last decades to overcome limitations related to conventional maintenance and repair methods. These materials have the ability to heal microcracks with less or no intervention, extending service life and safety of the components and reducing maintenance time and cost [4,5]. Several techniques have been used to produce self-healing composite materials. For epoxy matrix, one of the approaches used is the

incorporation of solid-state thermoplastic polymer as a healing agent into the thermoset matrix.

The thermoplastic healing agent must have melting point and viscosity that provide flow into the crack plane besides chemically reactive functional groups with the groups of the thermoset matrix. Good adhesive properties are also important to provide strong bonding with the matrix during crack repair [6]. When the material is heated up, the thermoplastic flows into the damaged areas, thus healing microcracks. Considering these requirements, several thermoplastic polymers have been investigated as healing agents for epoxy. Previous works suggest that poly (ethylene-co-methacrylic acid) acrylic thermoplastic (EMAA) is an efficient healing agent for epoxy-based composites [7–10].

The use of EMAA has been proposed as a healing agent capable of recovering fracture resistance on damaged epoxy after heated at 150 °C for 30 min [10]. For composites samples, the healing efficiency of the system is the result of plastic flow of the EMAA after heating, forming thin ligaments and joining the delaminated surfaces. These thermoplastic ligaments are capable of transferring the applied stress throughout the crack planes, increasing the interlaminar resistance of the system [11]. Typically, healing efficiency has been accessed based on fracture toughness of the composite material using double cantilever beam (DCB) and single edge notched bar (SENB) test specimens [6–9], showing increase of resistance to fatigue crack growth under mode I and

\* Corresponding author.

E-mail address: [allanaazevedon@hotmail.com](mailto:allanaazevedon@hotmail.com) (A. Azevedo do Nascimento).

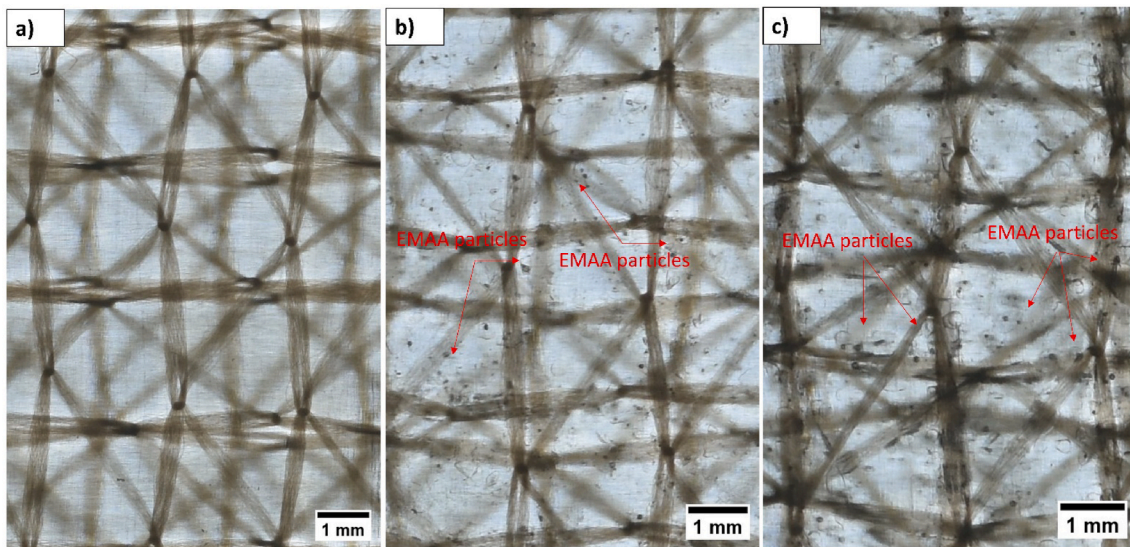


Fig. 1. Images of manufactured samples a) unmodified, b) E2% and c) E5% composites.

II cyclic loading and partial recover of the fatigue properties after healing cycle [12]. The healing efficiency of EMAA modified composites has also been studied using Paris model plots of cyclic strain energy release rate against delamination crack growth rate of DCB specimens, before and after healing [9].

Thus, self-healing composites using EMAA may be a promising approach for repair damages in these structures, minimizing damages caused by impact, fatigue and environmental factors, and repairing microcracks produced during operation. This approach can extend the service life of components and increase safety, while reducing time and costs associated with maintenance. However, further studies with self-healing glass-epoxy composites with the addition of EMAA are necessary considering the potential application of these materials for components of primary structures. A previous investigation of self-healing glass/epoxy composites using microvascular channels showed that addition of the healing agent creates zones of resin concentration and increase of fiber distortion angle, leading to the decrease of mechanical properties of the composites [13]. In this context, despite many investigations towards healing efficiency, a deeper understanding of the basic structural properties of self-healing materials is still necessary [14].

The present investigation evaluates self-healing glass fiber/epoxy composites with addition of poly (ethylene-co-methacrylic acid) (EMAA) under uniaxial cyclic tensile loading. Stress versus number of cycles to failure (S–N) curves were built for composites with two different contents of healing agent. The effects of the addition of EMAA on fatigue life of the composites was investigated and the self-healing efficiency was assessed through number of cycles to failure.

## 2. Experimental

### 2.1. Specimen preparation

Glass fiber/epoxy [0/90]<sub>s</sub> laminates with 2 mm thickness were manufactured using epoxy resin RIMR 135 and hardener RIMH 137 from Hexion in stoichiometric ratio 100:30 and unidirectional glass fibers UE 640 g/m<sup>2</sup> from Saertex, by Resin Transfer Molding (RTM).

Poly (ethylene-co-methacrylic acid) (EMAA) from Sigma-Aldrich was used for self-healing efficiency investigation. EMAA pellets were cryogenically ground and sieved into particles with size between 150 μm and 315 μm. Composites modified with EMAA contents of 2 wt% and 5 wt% were produced. The addition of 5 wt% of EMAA was previously found to promote self-healing ability in carbon fiber/epoxy composites

[15]. The EMAA contents evaluated in this study were chosen to achieve healing with minimum effect on the mechanical properties of the composites.

Modified laminates were manufactured with EMAA powder added between the layers of glass fibers before impregnation. After that, the mold was closed and heated up to 70 °C for 2 h to promote adhesion of the EMAA particles to the fibers and avoid displacement of the particles during resin flow. After 24 h, resin infusion was carried out at room temperature.

Unmodified laminate, without EMAA particles, was also manufactured using the same processing parameters for comparison. All laminates were cured for 48 h at room temperature, and post cured in an oven at 80 °C for 15 h, according to the cure cycle suggested by the manufacturer of the epoxy resin [16].

The fiber volume fractions  $V_f$  of the composites, measured according to ASTM D3171, were  $47.1\% \pm 1.1$ ,  $46.7\% \pm 0.9$  and  $46.9\% \pm 1.3$  for unmodified composites, EMAA 2 wt% and EMAA 5 wt% composites, respectively. Fig. 1 show images of samples produced with fair homogenous particles dispersion.

### 2.2. Quasi-static tensile tests

Quasi-static tensile tests were conducted on three groups of composite samples, to understand the effects of EMAA on the in-plane tensile properties of the laminates and determine tensile strength ( $\sigma_{max}$ ). Nominal dimensions of the specimens used were 200 mm (length), 100 mm (gage length), 20 mm (width) and 2 mm (thickness). Tabs were used to prevent grip-induced failures. The tests were carried out at room temperature ( $23 \pm 3$  °C) in a Schenk PSB servo-hydraulic testing machine with 63 kN load capacity. Loading rate of 2 mm/min was used and strain measurements were made using strain gauges at the center of each specimen. At least five specimens were tested for each sample. Tests were carried out following general recommendations of ASTM D3039 [17].

### 2.3. Fatigue tests

Specimens with same geometry as quasi-static specimens were tested in a Schenk PSB servo-hydraulic testing machine to evaluate in-plane material performance under a cyclic uniaxial tensile load. Tension-tension fatigue tests were carried out at room temperature ambient ( $23 \pm 3$  °C) in load control mode with frequency of 5 Hz and  $R = 0.1$  ( $\sigma_{min}/\sigma_{max}$ ). Three different load levels were used to investigate the

**Table 1**  
Mechanical properties of composite samples.

Samples	Tensile strength (MPa) $\mu$ (s) <sup>*</sup>	Modulus of elasticity (GPa) $\mu$ (s) <sup>*</sup>	Elongation at break (%) $\mu$ (s) <sup>*</sup>
Unmodified composites	466.1 (15.6)	23.5 (0.5)	2.6 (0.1)
E2% composites	466.6 (10.8)	24.2 (0.6)	2.7 (0.1)
E5% composites	449.9 (15.7)	23.9 (0.7)	2.7 (0.3)

Note 1: \*  $\mu$  = arithmetic mean. (s) = estimated standard deviation.

effects of the addition of EMAA on the fatigue properties of glass fiber/epoxy laminates. The results of static tests were used to determine the load levels used for fatigue tests. Three stress levels were used:  $\sigma_1 = 186.43$  MPa,  $\sigma_2 = 233.04$  MPa and  $\sigma_3 = 279.64$  MPa, corresponding to 40%, 50% and 60% of tensile strength of unmodified composites. The tests were carried out until failure of the specimen or until  $10^6$  cycles. General recommendations of ASTM D3479 were followed.

In addition, fatigue tests were used to investigate any healing effect promoted by the addition of thermoplastic particles. The tests were carried out using 50% of the tensile strength of unmodified composites. Specimens unmodified composites, EMAA 2 wt% and EMAA 5 wt% composites were tested under cyclic loading and two conditions at which loading was interrupted were considered: a) tests stopped at  $10^3$  cycles and b) tests stopped at  $10^4$  cycles. Then, the specimens were removed from the fatigue test machine, and heated up in an oven at 150 °C for 30 min. These healing cycle parameters were also used in previous studies published in the literature for EMAA as healing agent [8,10,18]. After that, the tests were resumed until specimens' failure. Fatigue life data of healed and virgin specimens were compared to investigate the healing effect.

Fatigue tests for stress levels  $\sigma_1$  and  $\sigma_3$ , 40% and 60% of tensile strength, respectively - were carried out two specimens whilst three specimens for each group - virgin and healed - were used for tests carried out at stress level  $\sigma_2$ .

For all fatigue tests, a testing setup using camera and background light was used to take photos of the specimens during the tests and to monitor the damage progression as described in a previous work [19]. Pictures were automatically taken every  $10^3$  cycles with the first picture taken before starting the tests. When illuminated with a bright background light, cracks reduce the translucence of the specimens, which can be used as a damage indicator [19,20]. Gray scale values can be used to describe the darkness of a pixel. The intensity (darkness) was quantified using 256 increments from 0 (black) to 255 (white) and the damage  $D$  was expressed in terms of change of intensity  $\Delta I$ , related to the intensity at the initial state  $I_0$ . These values were then used to calculate the damage progression according to Equation (1) [19]. The intensity of a damaged area ( $I$ ) and a reference area with constant intensity throughout the tests ( $I_{ref}$ ) were considered to assure that potential variations in the background light during the tests would not interfere with

the results.

$$D = 1 - \frac{I(N)}{I(0)} \cdot \frac{I_{ref}(0)}{I_{ref}(N)} \quad (1)$$

## 2.4. Dynamic mechanical analysis (DMA)

Dynamic Mechanical Analysis (DMA) measurements of specimens from the three groups of composites were carried out using a Netzsch DMA 242 C. The measurements were carried out in a three-point bending testing mode with a constant frequency of 1.0 Hz, over the temperature range of  $-50$  °C– $200$  °C, with a heating rate of 2 °C/min. Two specimens from each group were tested as recommended by ASTM D7028 [21].

## 3. Results

### 3.1. Tensile tests

Stress-strain behavior of specimens from unmodified and modified composites was evaluated using static tensile tests. In addition, the tensile strength measured for unmodified composites was used as a reference to define stress levels for the dynamic tensile tests. Results of the tensile tests are summarized in Table 1 and the stress-strain curves are shown in Fig. 2.

According to the results obtained, the addition of EMAA in contents of 2 wt% and 5 wt% did not produce any significant change in tensile strength or modulus of elasticity of the composite. The softening effect of the thermoplastic was previously found to decrease tensile and compressive properties of carbon fiber/epoxy laminates more significantly for composites with higher EMAA weight fractions (10 wt% and 15 wt%). Tensile and compressive properties of carbon fiber/epoxy composites have been described to decrease at linear rate with the increase of weight fraction of thermoplastic [18]. In this study, the results suggest that, when the thermoplastic is added in low concentration, the lower strength and stiffness properties of EMAA have minor impact and tensile properties are dominated by the major constituents (fiber and thermoset matrix).

The change in slope in the stress-strain curve (Fig. 2a) indicates failure of the [90] plies. In a [0/90] laminate, the 90° layers are known to fail first while the 0° layers hold the load until complete failure [22, 23]. After the failure of 90° plies, the laminate stiffness is reduced due to the presence of microcracks and fiber failure [24]. Thus, the failure of the 90° plies is seen as a knee point in stress-strain curve whilst the ultimate failure occurs at fracture strain of 0° fibers [25]. The addition of EMAA did not produce any change in the failure mode of the laminates.

### 3.2. Dynamic mechanical analysis (DMA)

Results of the dynamic mechanical analysis of unmodified and

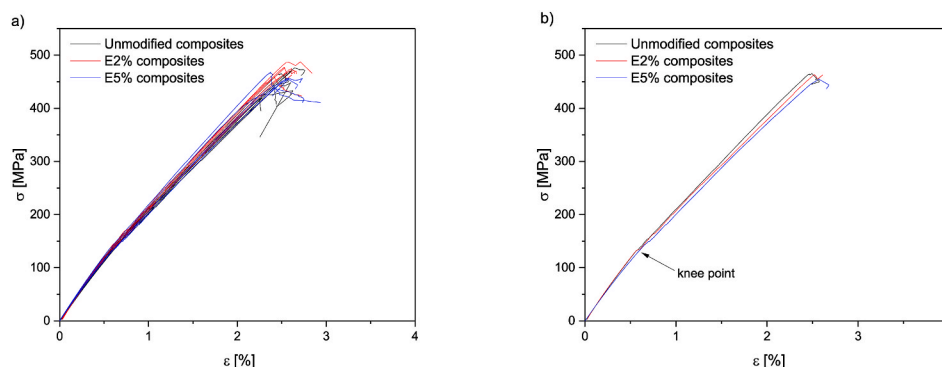


**Fig. 2.** Tensile stress versus strain of unmodified and modified samples a) all specimens and b) representative curves.

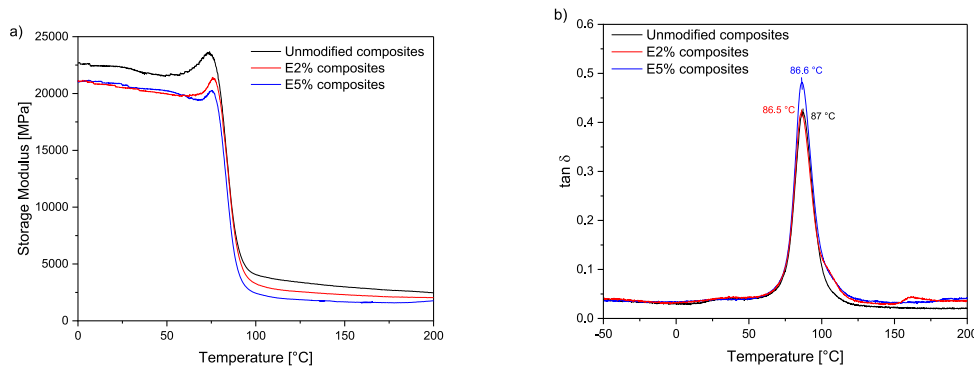


Fig. 3. DMA results for unmodified and modified composites a) Storage modulus and b) tan  $\delta$ .

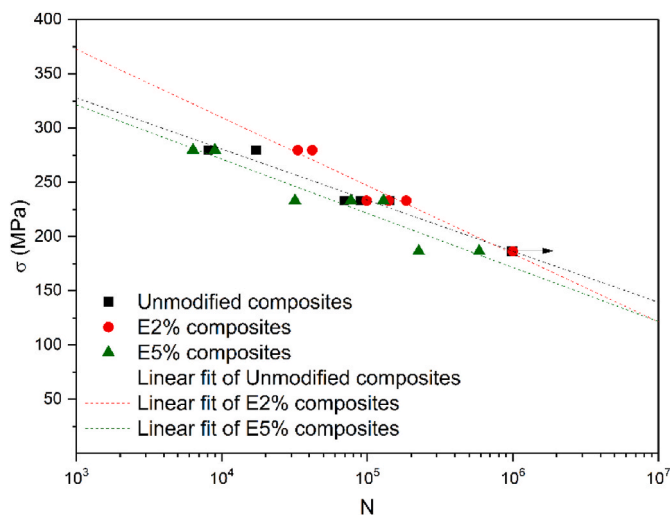


Fig. 4. S–N diagram for unmodified, EMAA 2% and EMAA5% composites.

modified composites are shown in Fig. 3. The peaks observed in storage modulus ( $E'$ ) (Fig. 3a), that precede the drop of glass transition ( $T_g$ ), for all samples is not unusual to be seen in curves for composites and are related with stress relief. With the increase of temperature, the molecules gain mobility to rearrange and release the stress introduced by the processing methods [26]. The storage modulus was not significantly affected by the addition of EMAA in contents of 2 wt% and 5 wt%. Moreover, the  $T_g$  of the composites were not affected by addition of EMAA. The  $T_g$ 's determined using the tan  $\delta$  peak (Fig. 3b) were 87.0 °C, 86.5 °C and 86.6 °C, for unmodified, E2% and E5% composites, respectively. In this case, the low content of EMAA used may not influence in the mobility of epoxy networks.

For EMAA/epoxy systems, the healing effect is the result of the viscous flow of EMAA into the crack plane. Thus, temperatures above the melting point of the thermoplastic are required for the healing mechanism to occur. However, temperatures above the  $T_g$  of the matrix have been used as healing temperature and are considered advantageous if no degradation of epoxy occurs [7,27]. For a healing temperature of 150 °C, above the  $T_g$  of the epoxy matrix, the mobility of polymer chains is expected to enhance the adhesion of the thermoplastic to the epoxy, thus improving healing.

### 3.3. Fatigue tests

Curves of maximum applied stress versus number of cycles to failure, known as S–N diagrams, were used to investigate the in-plane material

performance of unmodified and modified composites. Fig. 4 shows the S–N diagram for the three load levels tested. For  $\sigma_3$ , the lowest stress level, the specimens of unmodified composites and E2% composites did not fail and the tests were terminated at  $10^6$  cycles, as identified in S–N curve by an arrow mark. Comparing the fatigue life for unmodified and modified composites, the results suggest that the addition of 5 wt% of EMAA reduced the fatigue life of the laminates, while the addition of 2 wt% of EMAA promoted a slight increase in life.

The addition of EMAA increased initially the number of cycles to failure, which can be explained by interactions between the healing agent and micro-cracks. Strong interfacial adhesion between EMAA and epoxy has been reported and related to chemical bonding during curing and/or post-curing of the resin and it has been shown as important for the healing mechanism of this system [28,29]. These strong interfacial interactions may hinder matrix crack growth during loading, increasing the fatigue life of composites with 2 wt% of EMAA particles. In a previous work, EMAA filaments were found to increase the crack initiation and steady-state crack growth values of composites due to the high toughness of the thermoplastic, when compared with epoxy. Thus, the crack is pinned or deflected when the crack tip reaches the thermoplastic [30]. For cross-ply laminates under cyclic loading, transverse matrix cracks developing in the 90° layer and internal delaminations initiate at the tips of the cracks growing along the interface [31]. Then, EMAA particles might hinder the matrix cracking and consequently delamination, acting as barrier for damage.

However, with the increase in content of thermoplastic particles, the number of cycles to failure decreased. In this case, EMAA particles may behave as defects, which outweighs the positive effects of the adhesion epoxy/EMAA, decreasing the fatigue life of E5% composites. The increase of healing agent content was found to reduce mechanical properties of epoxy-based composites due several reasons, including fiber distortion, creation of resin-rich areas, agglomeration of healing agent which increase local stress distribution, hence reduce performance of the composite [13,32,33]. For E5% composites, the increase of the third component produced thermoplastic-rich areas (Fig. 1), which might act as flaws for damage initiation, reducing the fatigue life of the composite.

The increase in number of loading cycles is also known to cause loss of stiffness in fiber reinforced polymers. The dynamic stiffness during fatigue tests can be assessed by the normalized slope of the load-displacement (L–D) curve. Even though, the normalized L–D slope does not correspond to the stiffness of the specimens, the variation of the L–D slope represents the variation of stiffness and the curve is used to assess stiffness degradation during fatigue loading [34–36]. The L–D slope was calculated according to Equation (2) and normalized using the initial value of the slope as described by previous authors [37].

$$L = \frac{(L_{max} - L_{min})_{(n)}}{(D_{max} - D_{min})_{(n)}} \quad (2)$$

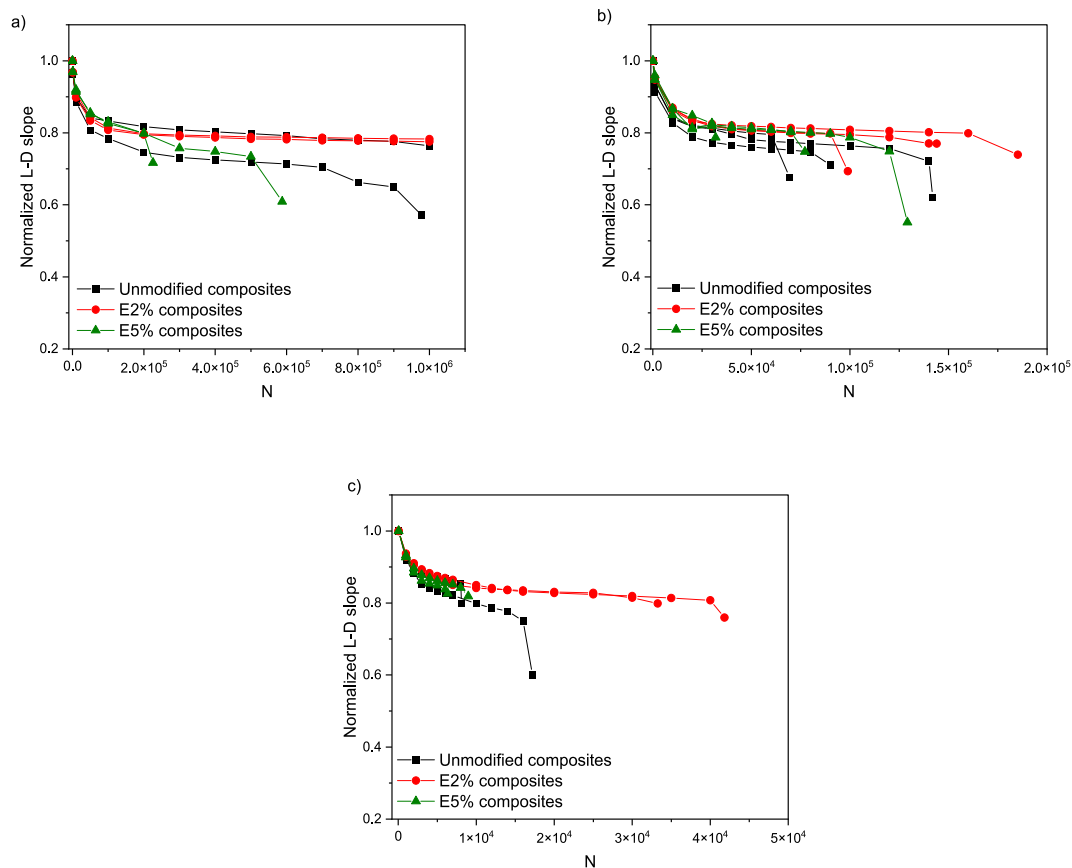


Fig. 5. Normalized L-D slope for Unmodified, E2% and E5% composites at stress levels a)  $\sigma_1 = 186.43$  MPa, b)  $\sigma_2 = 233.04$  MPa and c)  $\sigma_3 = 279.64$  MPa.

Where:

- $L$  is the L-D slope normalized to  $L_{(n = 1)}$ ;
- $L_{max}$  and  $L_{min}$  are the maximum and minimum load in one cycle, respectively;
- $D_{max}$  and  $D_{min}$  are the displacements corresponding to  $L_{max}$  and  $L_{min}$ , respectively.
- $n$  is the cycle index, from  $n = 1$  to  $n = N_{max}$ .

The normalized L-D slopes for unmodified and EMAA modified composites for  $\sigma_1$ ,  $\sigma_2$  and  $\sigma_3$  are shown in Fig. 5. The stiffness degradation process often occurs in three stages [25,38,39]. For the first few loading cycles, the stage I, a sharp drop in stiffness is observed, corresponding to the matrix cracking. Subsequently, a gradual reduction in stiffness at nearly constant rate is observed in stage II. In this stage, the growth of matrix cracks induces debonding and interlaminar failure resulting in reduction of stiffness. With further increase of the number of loading cycles, damage progression results in a third stage of stiffness loss with a sharp drop due to multiple fiber breakage and, ultimately, failure of the specimen [37,38].

Results suggest that the rate of stiffness loss was more sensitive to the addition of EMAA at higher stress levels. In addition, E2% composites presented lower stiffness loss when compared with unmodified composites samples and with E5% composites, in agreement with the increase of fatigue life observed in S-N diagrams, suggesting once again that the thermoplastic particles pinned the crack tips, thus delaying delamination growth.

The combination of fatigue life, residual stiffness and damage progression is often used to the understanding of fatigue damage mechanisms of laminates [38]. Therefore, damage progression was also investigated using photographs of the damage areas. In Fig. 6, curves of

damage ( $D\%$ , according to Equation (1)) vs. number of cycles to failure ( $N$ ) are shown. Results for damage evolution are in good agreement with results showed in S-N diagram (Fig. 4). The damage progresses sharply in the early stage of fatigue life, due to the multiple matrix cracking transverse to the load direction. As the number of load cycles increased, matrix cracking led to delaminations and loss of integrity of the laminate. The last stages of damage were characterized by extensive fiber breakage, as previously described in the literature [40,41].

The damage progression in E2% composites was reduced, as compared to the other samples, especially for higher stress levels.

### 3.4. Healing tests

For better understanding of the fatigue behavior and comparison of healing tests results, a linear fitting procedure was applied to fit the experimental results and used to estimate a reference number of cycles ( $N_{ref}$ ) for each group at stress level  $\sigma_2$ .

Numerous models have been developed to describe fatigue behavior of composites [42]. In this study, the experimental fatigue results were fitted using Equation (3) [38,39,42,43].

$$S = \sigma_{max}(a \log N + b) \tag{3}$$

Where:

- $S$  is the maximum applied stress;
- $\sigma_{max}$  is the tensile strength;
- $N$  is the number of cycles to failure;
- $a$  is the slope.

As the tensile strength of unmodified composites specimens was used to define the levels for the fatigue tests, the same value was used for all

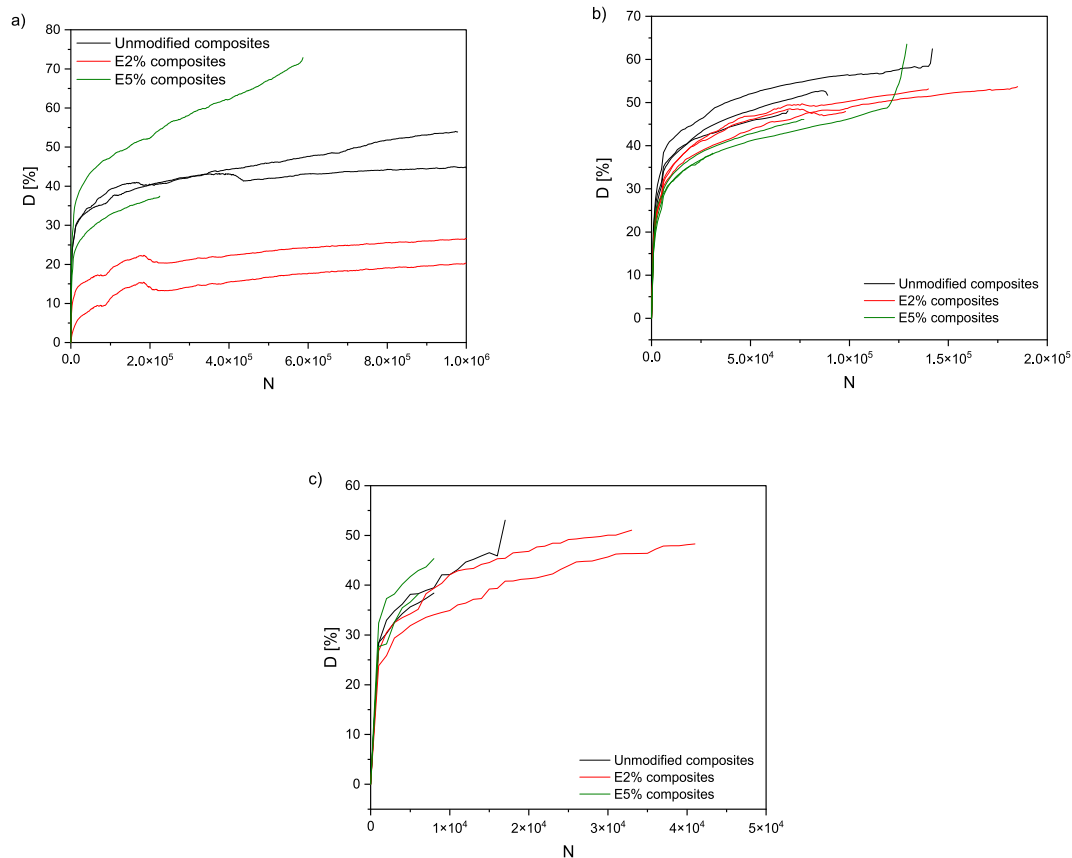


Fig. 6. Damage progression of unmodified and modified GFRP during fatigue tests at stress levels a)  $\sigma_1 = 186.43$  MPa, b)  $\sigma_2 = 233.04$  MPa and c)  $\sigma_3 = 279.64$  MPa.

**Table 2**  
Fitting parameters of S–N curve for unmodified and modified composites.

Sample	a	B	R <sup>2</sup>	N <sub>ref</sub>
Unmodified composites	−0.101	1.001	0.972	102724
E2% composites	−0.135	1.203	0.962	166674
E5% composites	−0.107	1.011	0.902	58674

curve fittings. The parameters *a* and *b* were calculated by least square regression analysis and are shown in Table 2. The fitted S–N diagrams for each group of specimens are shown in Fig. 7.

The R<sup>2</sup> values indicate that the regression equation fit well with the experimental data, since the values are close to unity. In addition, the fitting was used to estimate a reference value of load cycles (N<sub>ref</sub>) at stress level  $\sigma_{max} = 233.04$  MPa.

For stress level  $\sigma_2$ , the narrowest scatter was observed for unmodified composites, which also increased R<sup>2</sup> and the scatter was found to increase with EMAA content.

Values of N<sub>ref</sub> were used to calculate healing efficiency. The healing efficiency ( $\eta$ ) is used as measurement of the ability of the material to recover properties and was calculated as shown in Equation (4) [4,44]. Recovery ratios related to fracture stress and energy, mechanical properties and interlaminar strength have been used to estimate healing efficiency of fiber reinforced plastics [15,18,44]. This study proposes the use of number of cycles to failure (N) during the cyclic loading to estimate the healing efficiency of glass fiber/epoxy composites.

$$\eta = \frac{Property_{healed}}{Property_{initial}} \times 100 \tag{4}$$

Where:

*Property<sub>healed</sub>* is the number of cycles to failure after the healing cycle;  
*Property<sub>initial</sub>* is the N<sub>ref</sub> of each group calculated by regression analyses.

Results of fatigue life measurements for healing assessment are shown in Fig. 8. The average healing efficiency values are shown in Table 3. Specimens were tested until 10<sup>3</sup> (Fig. 8a) or 10<sup>4</sup> (Fig. 8b) cycles at the same stress level of  $\sigma_2$ , carefully removed from the test machine and then heated up in an oven for 30 min at 150 °C. The load cycles values presented in Fig. 8 correspond to the number of cycles to failure after the heating procedure.

According to the results presented in Table 3, the healing efficiency was higher when the specimen was subjected to heating after 10<sup>3</sup> loading cycles, suggesting that, at this stress level, the healing can be more efficient when activated in early stages of damage. In fact, in this case, self-healing mechanisms are intended to reverse matrix micro-cracks that, for cyclic loading, are known to be the first type of damage occurring in cross-ply laminates. Thus, while full recover or even increase in fatigue life was observed in specimens that the healing process was achieved by heating the material after 10<sup>3</sup> loading cycles, the healing efficiency was reduced to less than 40% when healing occurred after 10<sup>4</sup> loading cycles.

Results of healing efficiency for samples without thermoplastic addition showed complete recovery of fatigue life after the healing protocol applied at 10<sup>3</sup> loading cycles, suggesting that heating at the temperature of 150 °C, thus well above the Tg of 87 °C of the polymer matrix, allowed mobility of the polymer chains around the crack planes and crack tips, hence promoting post-cure and producing some healing-like effect.

For components during service, visual analysis and non-destructive testing (NDT) are used for inspection and damage analysis of the composite material. After detecting the damage, the repair is designed based

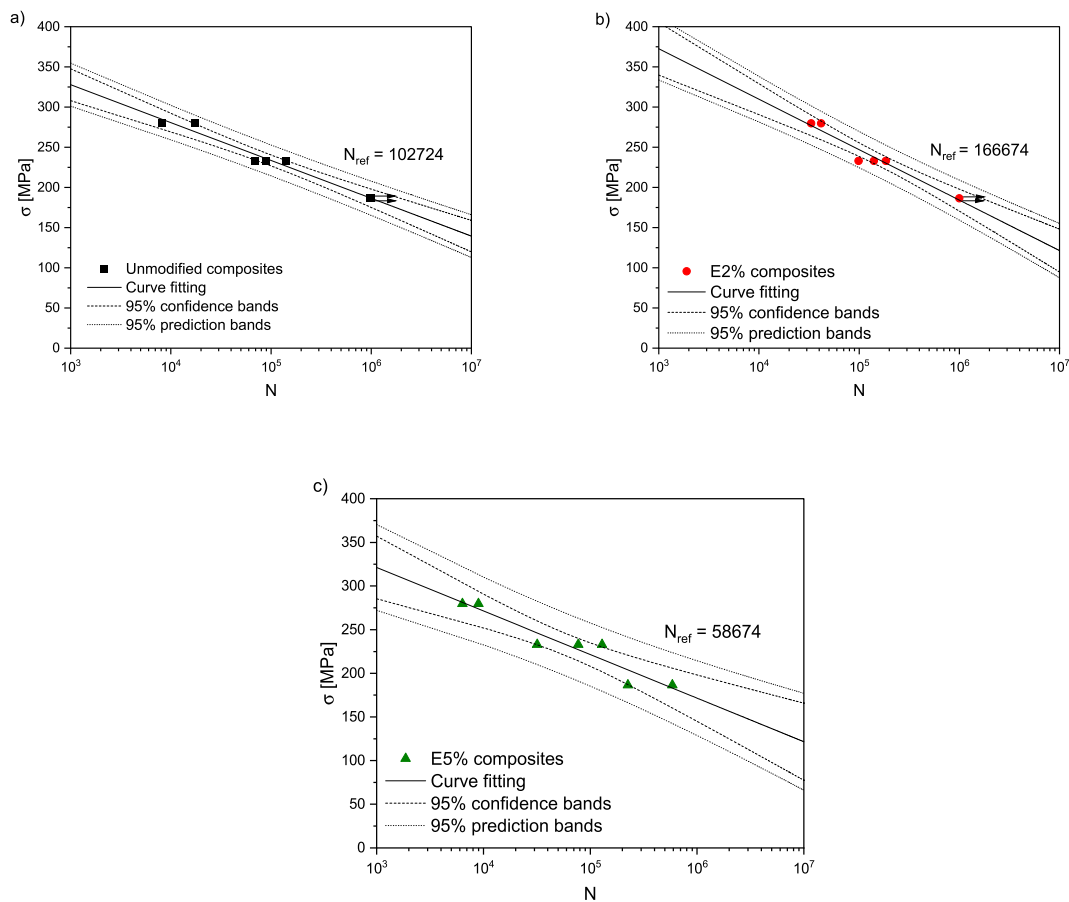


Fig. 7. S–N diagrams for a) unmodified composites, b) E2% composites and E5% composites with fitting function and confidence bands.

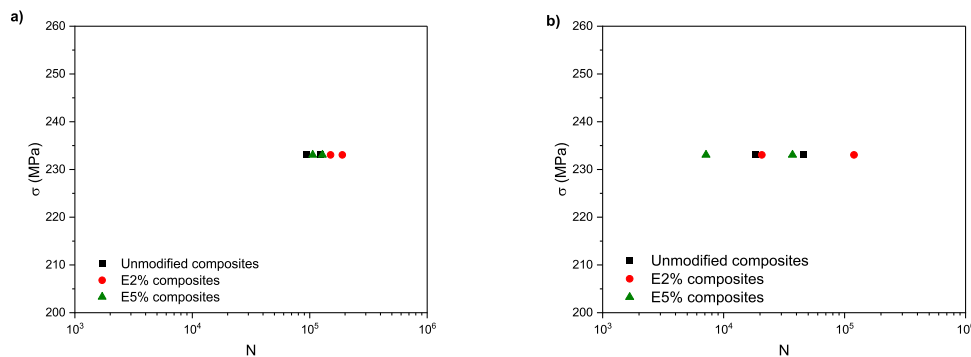


Fig. 8. S–N diagrams for healed specimens pre-loaded until a)  $10^3$  and b)  $10^4$  cycles.

**Table 3**  
Average healing efficiency of unmodified and modified composites.

Sample	$\eta$ (%)	
	$10^3$	$10^4$
Unmodified composites	105.9	31.2
E2% composites	102.1	27.4
E5% composites	199.6	37.7

on several criteria, such as the type of damage found and availability of resources. For on-site repair, the application of localized heating at elevated temperatures is a common practice to promote the cure of

epoxy resin during repair techniques [45,46]. Therefore, the results obtained in this study suggest that the addition of EMAA may be a promising approach to produce composite materials for structural applications with self-healing capability, which will result in increased fatigue life.

Complete recovery of fatigue life was also observed in composites with the addition of 2 wt% of EMAA. These were the specimens with longer fatigue life when tested under cyclic loading in pristine conditions ( $N_{ref}$ ), 60% higher than for unmodified specimens and 2.8 times the fatigue life of specimens with the addition of 5 wt% of EMAA. Thus, the number of cycles to failure of composites with 2 wt% of EMAA was the greatest among all healed materials, even though the healing efficiency was lower than for composites with 5 wt% of EMAA.

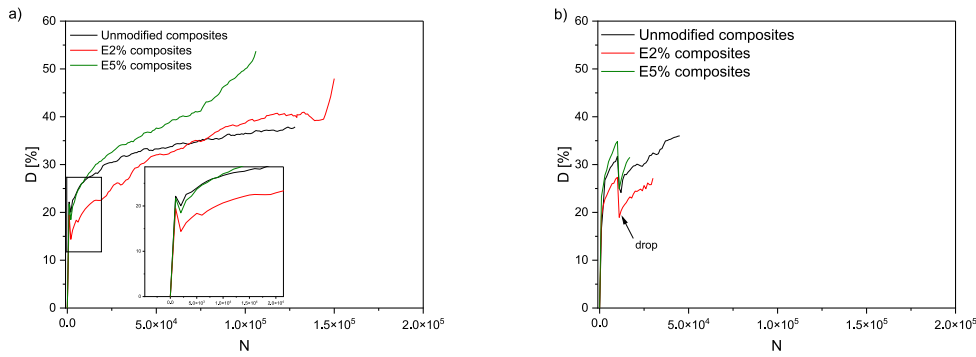


Fig. 9. Damage evolution before and after healing for unmodified and modified composites tested until a)  $10^3$  and b)  $10^4$  loading cycles before heating.

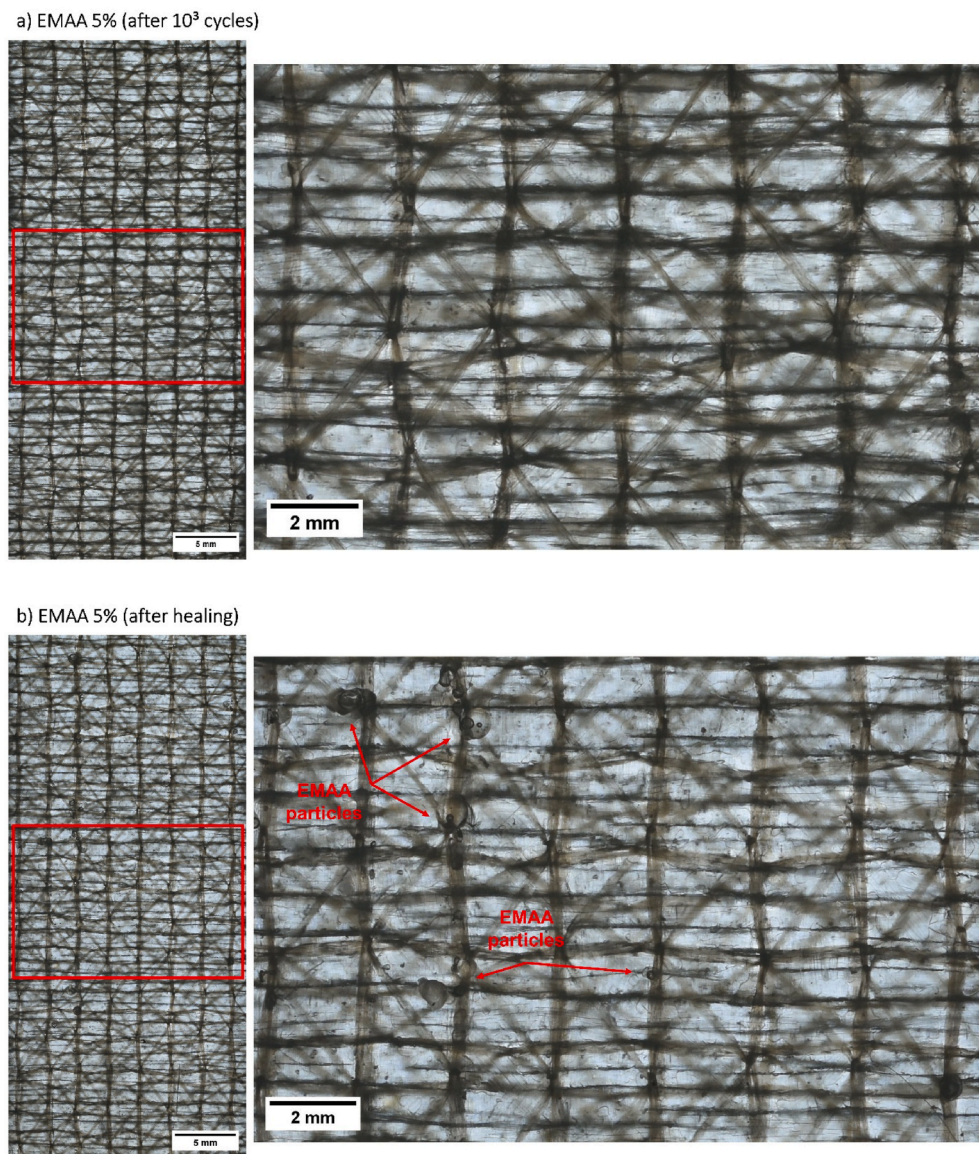


Fig. 10. E5% composites sample tested until  $10^3$  a) before heating and b) after heating.

Increasing the content of EMAA from 2 wt% to 5 wt%, the self-healing efficiency increased, the ability of EMAA to recover fatigue life of glass fiber/epoxy composites. However, since the fatigue life of

pristine specimens with the addition of 5 wt% of EMAA was lower than for 2 wt% of EMAA, the number of cycles to failure for this healed material was lower than that of 2 wt% of EMAA.



Besides the healing efficiency, damage progression evaluation was carried out for specimens under healing tests. Pictures were taken during the first stage of load cycles and after the healing protocol to assess the effect of EMAA on damage stage of the composites. Curves  $D \times N$  are shown in Fig. 9. A drop in the curves is observed at  $10^3$  cycles (Figs. 9a) and  $10^4$  cycles (Fig. 9b), i.e., the moment when the test was interrupted and the healing protocol was carried out, before the cyclic loading was resumed. The drop indicates the reduction in damage state after the heating, thus corroborating the healing effect.

Fig. 10 shows images of E5% composites after  $10^3$  cycles and after heating. The thermoplastic healing agent is observed in damaged areas after the healing process. During heating, the EMAA melting promotes the flow of the thermoplastic into the damaged areas, thus rebinding adjacent crack planes (Fig. 10b) [9].

#### 4. Conclusions

In this work, the potential of EMAA as healing agent for glass fiber/epoxy composites was investigated. Composites with 2 wt% and 5 wt% of EMAA were manufactured by resin infusion using glass fibers impregnated with EMAA. Healing efficiency was evaluated based on number of cycles to failure of specimens subjected to cyclic loading. The addition of EMAA did not produce any significant effect on glass transition temperature, tensile strength or modulus of elasticity of the composites. However, the results suggest that the addition of 5 wt% of EMAA reduced the fatigue life of the laminates, while the addition of 2 wt% of EMAA promoted a slight increase in life. The number of cycles to failure of composites with 2 wt% of EMAA was also the greatest among all healed materials. The greatest healing efficiency was observed for specimens subjected to heating after  $10^3$  loading cycles, as compared to  $10^4$  loading cycles, suggesting that, the healing can be more efficient if activated in early stages of damage. Overall, this work contributed to the understanding of the effects of EMAA as a healing agent to glass fiber/epoxy composites.

#### Author statement

Allana Azevedo do Nascimento: Investigation, Methodology, Formal analysis, Writing – original draft.

Ana Paula Cysne Barbosa: Conceptualization, Validation, Supervision.

Volker Trappe: Validation, Supervision, Resources.

José Daniel Diniz Melo: Project administration, Validation, Writing – revision & editing.

#### Declaration of competing interest

The authors declare that they have no known competing financial interests or personal relationships that could have appeared to influence the work reported in this paper.

#### Acknowledgements

This study was financed in part by the Coordenação de Aperfeiçoamento de Pessoal de Nível Superior - Brasil (CAPES) - Finance Code 001 and PrInt/CAPES.

#### References

- [1] A.S. Rahman, Design of cost-effective and efficient fiber-reinforced composite blades for wind turbines, *Reinforc Plast* 63 (1) (2019) 21–25.
- [2] R.M. Novais, J. Carvalheiras, M.N. Capela, M.P. Seabra, R.C. Pullar, J.A. Labrincha, Incorporation of glass fibre fabrics waste into geopolymer matrices: an eco-friendly solution for off-cuts coming from wind turbine blade production, *Construct. Build. Mater.* 187 (2018) 876–883.
- [3] L. Mishnaevsky, K. Branner, H.N. Petersen, J. Beauson, M. McGugan, B.F. Sørensen, Materials for wind turbine blades: an overview, *Materials* 10 (11) (2017) 1–24.
- [4] P.S. Tan, A.A. Somashekar, P. Casari, D. Bhattacharyya, Healing efficiency characterization of self-repairing polymer composites based on damage continuum mechanics, *Compos. Struct.* 208 (September 2018) (2019) 367–376.
- [5] I.L. Hia, V. Vahedi, P. Pasbakhsh, Self-healing polymer composites: prospects, challenges, and applications, *Polym. Rev.* 56 (2) (2016) 225–261.
- [6] I.L. Hia, V. Vahedi, P. Pasbakhsh, Self-healing polymer composites: prospects, challenges, and applications, *Polym. Rev.* 56 (2) (2016) 225–261.
- [7] R.J. Varley, D.A. Craze, A.P. Mouritz, C.H. Wang, Thermoplastic healing in epoxy networks: exploring performance and mechanism of alternative healing agents, *Macromol. Mater. Eng.* 298 (11) (2013) 1232–1242.
- [8] K. Pingkarawat, C. Dell'Olio, R.J. Varley, A.P. Mouritz, An efficient healing agent for high temperature epoxy composites based upon tetra-glycidyl diamino diphenyl methane, *Compos. Appl. Sci. Manuf.* 78 (2015) 201–210.
- [9] S. Meure, S. Furman, S. Khor, Poly[ethylene-co-(methacrylic acid)] healing agents for mendable carbon fiber laminates, *Macromol. Mater. Eng.* 295 (5) (2010) 420–424.
- [10] S. Meure, D.Y. Wu, S. Furman, Polyethylene-co-methacrylic acid healing agents for mendable epoxy resins, *Acta Mater.* 57 (14) (2009) 4312–4320.
- [11] K. Pingkarawat, T. Bhat, D.A. Craze, C.H. Wang, R.J. Varley, A.P. Mouritz, Healing of carbon fibre-epoxy composites using thermoplastic additives, *Polym. Chem.* 4 (18) (2013) 5007–5015.
- [12] R.B. Ladani, C.H. Wang, A.P. Mouritz, Delamination fatigue resistant three-dimensional textile self-healing composites, *Compos. Appl. Sci. Manuf.* 127 (2019), 105626.
- [13] M.A. Mohammadi, R. Eslami-Farsani, H. Ebrahimnezhad-Khaljiri, Experimental investigation of the healing properties of the microvascular channels-based self-healing glass fibers/epoxy composites containing the three-part healant, *Polym. Test.* 91 (2020), 106862.
- [14] M. Scheiner, T.J. Dickens, O. Okoli, Progress towards self-healing polymers for composite structural applications, *Polymer* 83 (2016) 260–282.
- [15] A.A. do Nascimento, F. Fernandez, F.S. da Silva, E.P.C. Ferreira, J.D. José, A. P. Cysne Barbosa, Addition of poly (ethylene-co-methacrylic acid) (EMAA) as self-healing agent to carbon-epoxy composites, *Compos. Appl. Sci. Manuf.* 137 (February) (2020), 106016.
- [16] Momentive, "Product Specification - EPIKOTE RESIN MGS RIMR426," vol. 49, no. 0, pp. 1–8.
- [17] ASTM, Annual Book of ASTM Standards, 2014, pp. 1–13. *Astm D3039/D3039M*.
- [18] K. Pingkarawat, C.H. Wang, R.J. Varley, A.P. Mouritz, Mechanical properties of mendable composites containing self-healing thermoplastic agents, *Compos. Appl. Sci. Manuf.* 65 (2014) 10–18.
- [19] D. Kraus, V. Trappe, Transverse damage in glass fiber reinforced polymer under thermo-mechanical loading, *Composites Part C: Open Access* 5 (2021), 100147.
- [20] A. Müller, V. Trappe, S. Hickmann, H.-P. Ortwein, Investigation of the infinite life of fibre-reinforced plastics using X-ray refraction topography for the in-situ, non-destructive evaluation of micro-structural degradation processes during cyclic fatigue loading, in: *Fatigue of Materials at Very High Numbers of Loading Cycles*, 2018, pp. 417–439.
- [21] ASTM International, ASTM D7028-07 - Standard Test Method for Glass Transition Temperature (DMA Tg) of Polymer Matrix Composites by Dynamic Mechanical Analysis (DMA), 2012.
- [22] C. Ghafafian, B. Popiela, V. Trappe, Failure mechanisms of GFRP scarf joints under tensile load, *Materials* 14 (7) (2021) 1806.
- [23] O. Gunes, Developments in Fiber-Reinforced Polymer (FRP) Composites for Civil Engineering, 2013.
- [24] S.W. Tsai, J.D.D. Melo, Composite Materials Design and Testing, *Composites Design Group*, 2015.
- [25] N.H. Padmaraj, K.M. Vijaya, P. Dayananda, Experimental study on the tension-tension fatigue behaviour of glass/epoxy quasi-isotropic composites, *J. Eng. Sci. King Saud Univ.* 32 (6) (2020) 396–401.
- [26] K.P. Menard, N. Menard, Dynamic mechanical analysis, *Encyclopedia of Analytical Chemistry* (2017) 1–22.
- [27] K. Pingkarawat, C. Dell'Olio, R.J. Varley, A.P. Mouritz, Poly(ethylene-co-methacrylic acid) (EMAA) as an efficient healing agent for high performance epoxy networks using diglycidyl ether of bisphenol A (DGEBA), *Polymer* 92 (2016) 153–163.
- [28] S. Meure, D.Y. Wu, S.A. Furman, FTIR study of bonding between a thermoplastic healing agent and a mendable epoxy resin, *Vib. Spectrosc.* 52 (1) (2010) 10–15.
- [29] S. Meure, R.J. Varley, D.Y. Wu, S. Mayo, K. Nairn, S. Furman, Confirmation of the healing mechanism in a mendable EMAA-epoxy resin, *Eur. Polym. J.* 48 (3) (2012) 524–531.
- [30] T.W. Loh, R.B. Ladani, A. Ravindran, R. Das, E. Kandare, A.P. Mouritz, Z-Pinned composites with combined delamination toughness and delamination Self-Repair properties, *Compos. Appl. Sci. Manuf.* 149 (June) (2021), 106566.
- [31] N.V. Akshantala, R. Talreja, A micromechanics based model for predicting fatigue life of composite laminates, *Mater. Sci. Eng.* 285 (2000) 303–313.
- [32] H. Ebrahimnezhad-Khaljiri, R. Eslami-Farsani, The tensile properties and interlaminar shear strength of microcapsules-glass fibers/epoxy self-healable composites, *Eng. Fract. Mech.* 230 (2020), 106937.
- [33] M.A. Mohammadi, R. Eslami-Farsani, H. Ebrahimnezhad-Khaljiri, Experimental investigation of the healing properties of the microvascular channels-based self-healing glass fibers/epoxy composites containing the three-part healant, *Polym. Test.* 91 (July) (2020), 106862.
- [34] M. Karahan, S.V. Lomov, A.E. Bogdanovich, I. Verpoest, Fatigue tensile behavior of carbon/epoxy composite reinforced with non-crimp 3D orthogonal woven fabric, *Compos. Sci. Technol.* 71 (16) (2011) 1961–1972.

- [35] V. Carvelli, V.N. Tomaselli, S.V. Lomov, I. Verpoest, V. Witzel, B. Van den Broucke, Fatigue and post-fatigue tensile behaviour of non-crimp stitched and unstitched carbon/epoxy composites, *Compos. Sci. Technol.* 70 (2010) 2216–2224.
- [36] B. Yu, R.S. Bradley, C. Soutis, P.J. Hogg, P.J. Withers, 2D and 3D imaging of fatigue failure mechanisms of 3D woven composites, *Compos. Appl. Sci. Manuf.* 77 (2015) 37–49.
- [37] L. Guo, J. Huang, L. Zhang, X. Sun, Damage evolution of 3D woven carbon/epoxy composites under tension-tension fatigue loading based on synchrotron radiation computed tomography (SRCT), *Int. J. Fatig.* 142 (2021), 105913.
- [38] N.H. Padmaraj, K.M. Vijaya, P. Dayananda, Experimental investigation on fatigue behaviour of glass/epoxy quasi-isotropic laminate composites under different ageing conditions, *Int. J. Fatig.* 143 (July 2020) (2021), 105992.
- [39] P.R. Vieira, E.M.L. Carvalho, J.D. Vieira, R.D. Toledo Filho, Experimental fatigue behavior of pultruded glass fibre reinforced polymer composite materials, *Compos. B Eng.* 146 (May 2017) (2018) 69–75.
- [40] R. Talreja, C.V. Singh, 11, *Damage and Failure of Composite Materials*, 6, Cambridge University Press, 2012.
- [41] O. Castro, P.A. Carraro, L. Maragoni, M. Quaresimin, Fatigue damage evolution in unidirectional glass/epoxy composites under a cyclic load, *Polym. Test.* 74 (2019) 216–224.
- [42] I. Burhan, H.S. Kim, S-N curve models for composite materials characterisation: an evaluative review, *J. Compos. Sci.* 2 (38) (2018).
- [43] X. Zhao, X. Wang, Z. Wu, Z. Zhu, Fatigue behavior and failure mechanism of basalt FRP composites under long-term cyclic loads, *Int. J. Fatig.* 88 (2016) 58–67.
- [44] D.Y. Wu, S. Meure, D. Solomon, Self-healing polymeric materials: a review of recent developments, *Prog. Polym. Sci.* 33 (5) (2008) 479–522.
- [45] L. Mishnaevsky, Repair of wind turbine blades: review of methods and related computational mechanics problems, *Renew. Energy* 140 (2019) 828–839.
- [46] D.J. Lekou, P. Vionis, Report on Repair Techniques for Composite Parts of Wind Turbine Blades, *Optimat Blades*, 2002, pp. 1–15.